

Patterns in open vent, strombolian behavior at Fuego volcano, Guatemala, 2005–2007

John J. Lyons · Gregory P. Waite · William I. Rose · Gustavo Chigna

Received: 20 November 2008 / Accepted: 17 June 2009
© Springer-Verlag 2009

Abstract Fuego volcano, Guatemala is a high (3,800 m) composite volcano that erupts gas-rich, high-Al basalt, often explosively. It spends many years in an essentially open vent condition, but this activity has not been extensively observed or recorded until now. The volcano towers above a region with several tens of thousands of people, so that patterns in its activity might have hazard mitigation applications. We conducted 2 years of continuous observations at Fuego (2005–2007) during which time the activity consisted of minor explosions, persistent degassing, paroxysmal eruptions, and lava flows. Radiant heat output from MODIS correlates well with observed changes in eruptive behavior, particularly during abrupt changes from passive lava effusion to paroxysmal eruptions. A short-period seismometer and two low-frequency microphones installed during the final 6 months of the study period recorded persistent volcanic tremor (1–3 Hz) and a variety of explosive eruptions. The remarkable correlation between seismic tremor, thermal output, and daily observational data defines a pattern of repeating eruptive behavior: 1) passive lava effusion and subordinate strombolian explosions, followed by 2) paroxysmal eruptions that produced sustained eruptive columns, long,

rapidly emplaced lava flows, and block and ash flows, and finally 3) periods of discrete degassing explosions with no lava effusion. This study demonstrates the utility of low-cost observations and ground-based and satellite-based remote sensing for identifying changes in volcanic activity in remote regions of underdeveloped countries.

Keywords Fuego · Guatemala · Strombolian · Paroxysmal · Seismo-acoustic · Open vent

Introduction

Fuego is a stratovolcano (3,800 m) with a well-defined summit crater which marks the southernmost expression of the north–south trending Fuego-Acatenango volcanic complex. It is located in Central Guatemala, within the second of eight segments of the Central American volcanic front (Carr et al. 2002; Fig. 1). Fuego has had at least 60 historical subplinian eruptions and several longer periods (i.e., months to years) of low-level strombolian activity. The most recent intense, subplinian activity (VEI 4), which occurred in four main pulses during October 1974, produced ash fall, pyroclastic flows, lava flows, and lahars that displaced local populations and damaged agricultural production (Rose et al. 1978). Low-level strombolian activity persisted until 1979 (Martin and Rose 1981) and from 1980 to 1999 Fuego had irregularly spaced subplinian (VEI 1–2) events with periods of repose (Smithsonian Institution 1979, 1999). The most recent continuous low-level strombolian activity began with a VEI 2 eruption on May 21, 1999, (Lyons et al. 2007; Smithsonian Institution 1999) and continued to the time of this writing (November 2008). This current activity is characterized by frequent, short (hundreds of meters) lava flows, pyroclastic explo-

Editorial responsibility: J. Stix

J. J. Lyons (✉) · G. P. Waite · W. I. Rose
Department of Geological Engineering and Sciences,
Michigan Technological University,
1400 Townsend Drive,
Houghton, MI 49931, USA
e-mail: jlyons@mtu.edu

G. Chigna
Instituto Nacional de Sismología, Vulcanología,
Meteorología e Hidrología,
7a Avenida 15-47 Zona 13,
Guatemala City, Guatemala

sions, lahars, and paroxysmal, extended-duration (i.e., 24–48 h) eruptions that produce longer lava flows (hundreds to thousands of meters), pyroclastic flows, and sustained eruptive columns. This more-or-less continuous activity leads to small eruptions nearly every day and a condition we call “open vent”, indicating that the vertical conduit, which has been the main vent in nearly all historic activity at Fuego, does not get constricted or plugged.

Within the historic record, the current activity is analogous to a period of low-level strombolian activity following the October 1974 eruption and lasting until 1979. Martin's (1979) thorough review of the historic record revealed that periods of persistent low-level activity are not common at Fuego. Unfortunately observations in the 1974–79 period were not detailed enough to make closer comparisons with 1999–2008.

Fuego has produced primarily high-Al basalt (~51% SiO₂) since 1974. Melt inclusions (MI) in erupted olivine indicate that Fuego's magmas, like many other arc basalts and basaltic andesites, contain dissolved H₂O concentrations ranging from 2.1 wt% to 6.1 wt% (Sisson and Layne 1993; Roggensack 2001). Studies of recently erupted tephra at Stromboli and Etna found ~50% SiO₂ and 2.8% H₂O (MI) in high-K basalts (Métrich et al. 2001) and ~47% SiO₂ and 2.5 to 3.4 wt% H₂O (MI) in alkali basalts (Métrich et al. 2004), respectively. The high volatile content of Fuego's magmas probably influences eruptive behavior during periods when an open vent condition dominates. Persistent basaltic activity has been observed and documented at other volcanoes worldwide (e.g., Stromboli, Kilauea, Etna, Arenal), but not thoroughly at Fuego. This paper presents a summary of the continuous eruptive activity at Fuego volcano from August 2005 to June 2007. We describe the observed activity and its cyclic nature, and present new, complementary geophysical and satellite data that provide quantitative support for our observations.

Background

From August 2005 through June 2007 we made nearly continuous observations of Fuego's eruptive behavior from a local observatory manned by the Guatemalan governmental organization responsible for volcano monitoring, the Instituto Nacional de Sismología, Vulcanología, Meteorología e Hidrología (INSIVUMEH). The observatory has a direct line of sight to the active summit of Fuego and is ~7.5 km southwest of the vent at 1,090 m elevation (Fig. 1). A single short-period seismometer and two low-frequency microphones were installed near the observatory and recorded from January 2007 to July 2007 to supplement daily observations (Fig. 1).

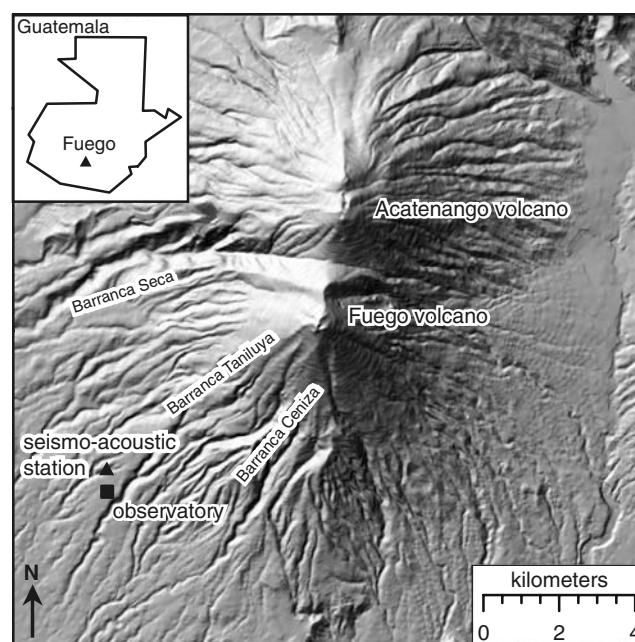


Fig. 1 Digital elevation model of the Fuego-Acatenango volcanic complex created from 1954 aerial photos. The seismo-acoustic station deployed from January–July 2007 was located 7 km southwest of the active summit of Fuego. Barrancas control emplacement of lava flows, lahars, pyroclastic flows, and rock fall. Elevation difference between the summit of Fuego and the observatory is ~2,700 m

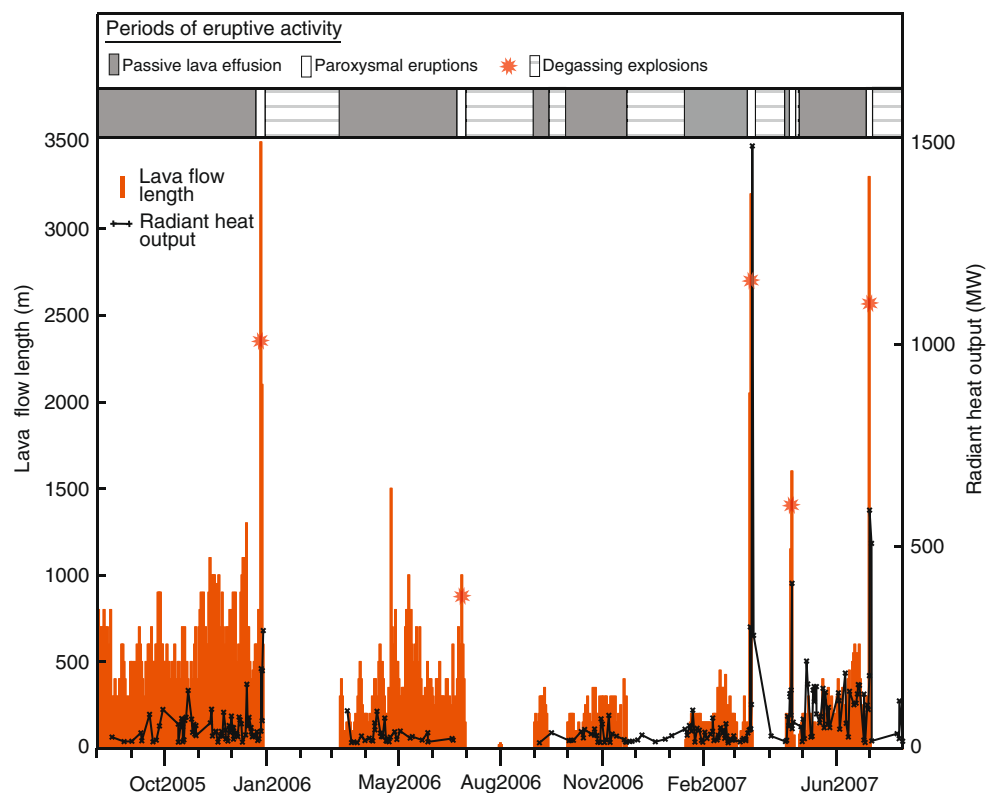
On the basis of our observations we classify the eruptive behavior observed into three categories: 1) lava effusion and subordinate strombolian explosions, 2) paroxysmal, extended-duration eruptions, and 3) periods of discrete, often pyroclastic, explosions with no concurrent lava effusion. The three types of activity were observed to occur in an ordered, repeating cycle of lava effusion and strombolian explosions, followed by a paroxysmal eruption, and finally explosions with no lava effusion. The complete cycle was observed five times during the 2-year observation period and two complete cycles were sampled during 2007 with the seismo-acoustic station.

Descriptions of observed eruptive behavior

Passive lava effusion and subordinate strombolian explosions

Lava flowed from the summit crater into one or more of the incised canyons distributed around the southern half of the volcano for more than half of the period of 2005–2007 (Figs. 1, 2). Long periods (days to weeks) of low output effusion alternated with short periods (hours to days) of high output effusion, which occurred only during the

Fig. 2 Observed daily lava flow lengths of all active lava flows (orange) and total radiant heat output in MW (black) calculated from MODVOLC acquisitions of nighttime MODIS data (Wright et al. 2004). The three distinct periods of activity identified by observations are also plotted (bar, above). Note the repeating pattern, 1) passive effusion, 2) paroxysmal eruption, 3) degassing explosions. The first period of passive effusion was ongoing at the start of this study, and the ultimate period of degassing explosions continued after the end of this study



paroxysmal eruptions described below. Typical lava flow dimensions during the low-rate effusive periods are 50–400 m long by 20–50 m wide and 2–4 m thick. These estimates were made on the basis of visual observations and field measurements of older accessible flows. The active flows were inaccessible due to the short lengths of the flows, steep slope and instability of the upper edifice, and the hazard from rock falls. Aerial observations of the summit region of Fuego show that some proximal lava flows have a pahoehoe texture, whereas an accessible portion of a particularly long flow (~4,000 m) from 2003 in the Taniluya canyon shows that distal lava flows are exclusively 'a'a. This suggests that Fuego lava flows convert to 'a'a during flow down steep barrancas. At night the lava flows are incandescent and clearly visible from the observatory. The majority of a flow would appear as dull orange ribbons and patches of incandescent lava within a black matrix of chilled lava (Fig. 3).

When effusive activity began, lava flows originating from Fuego's summit crater were coherent for several tens of meters down slope and lengthened to as much as several hundreds of meters within a period of hours to days. It was most common for a lava flow to grow for a period of several days or weeks before reaching a steady state, after which the front neither advanced nor retreated significantly for periods of weeks to months. Observations and infrared images suggest that the nearly constant flow lengths were preserved through a balance of magma flux into the flow

and lava calving from the sides and nearly fixed front of the flow (Fig. 3).

When output rate was relatively low, lava flow lengths changed slowly; however, during the paroxysmal eruptions (discussed below) the lava flows grew to ≥ 500 m in less than 24 h. The long, rapidly emplaced flows were short-lived, suggesting that effusive intensity, and thus magma flux, is sometimes highly variable at Fuego over short timescales, similar to activity at other basaltic systems such as Kilauea (Parfitt and Wilson 1994), Etna (Lautze et al. 2004), and Stromboli (Calvari et al. 2005).

Minor strombolian explosions

Fuego produced many hundreds of explosions during lava effusion in a style best classified as *strombolian* (Blackburn et al. 1976). The explosion clouds rose 50–500 m above the summit and varied widely in ash content. The explosions were often silent when observed from 7–10 km or produced a weak to moderate popping noise infrequently accompanied by a weak shock wave that would rattle windows and metal roofs. When observed at night, the explosions sprayed incandescent magma up to 100 m above the crater and provoked small incandescent rock falls around the summit. The frequency of explosions varied from none to several tens per hour; often explosions came in series, with the strongest explosion first, followed tens of seconds later by one or more weaker explosions.

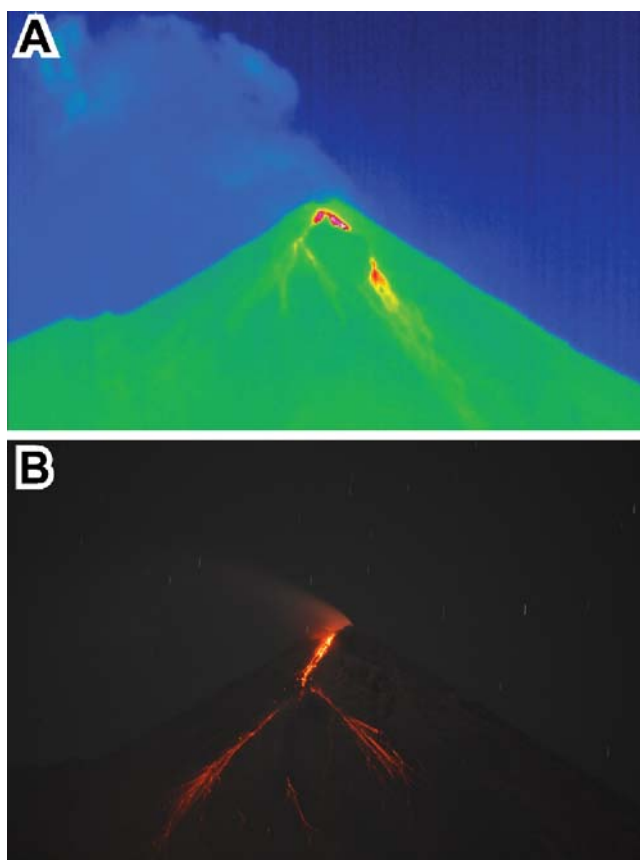


Fig. 3 Thermal IR imagery (14 January 2007) and photograph (26 February 2007) taken from the observatory of short (~100 m and 300 m, respectively) lava flows emanating from the summit crater of Fuego. IR image from an Infratec Variocam camera operating in the wavelength range 8–13.5 μm with an image resolution of 320×240 pixels. Note that a portion of the lava flow in the thermal image is obscured by a large bulge of old lava that sits high on the SW flank of Fuego. Both images illustrate how passive lava flows at Fuego maintain short lengths over weeks to months by shedding blocks of lava from the flow front and sides (thermal image courtesy of Nick Varley)

Degassing during lava effusion

Audible degassing from Fuego, observed 7–10 km from the vent, occurred predominately during periods of lava effusion and was manifest as two distinct noises, best described as ‘chugs’ and ‘jetting’. The chugging sounded very similar to the noise of a steam locomotive, with individual chugs occurring once every 1–4 s. The duration of the chugging varied from several seconds to tens of minutes of continuous chugging and chugging intensity varied from barely discernable to audible over almost all anthropogenic noise. Intensity would sometimes vary within individual sets of chugs, typically with faint chugging building to stronger chugs. When observed at night, chugging or jetting was often associated with minor incandescent ejecta and preceded increased lava flow activity (incandescence in the flow front and sides and more abundant rock fall) by a few minutes.

Chugging has been documented at many volcanoes that have similar activity and magmatic and volatile contents as Fuego, including Langila (Mori et al. 1989), Semeru (Schlindwein et al. 1995), Arenal (Benoit and McNutt 1997), Karymsky (Johnson and Lees 2000), and Sangay (Johnson 2007; Lees and Ruiz 2008). Benoit and McNutt (1997) attributed chugging to rhythmic degassing of a gas-charged magma. Johnson and Lees (2000) and Lees and Ruiz (2008) observed a linear correlation between explosion pressure and interexplosion time; they favor a model where pressure accumulates within a clogged conduit and is episodically vented. At Fuego, the chugging seems to represent more energetic degassing or a specific vent condition, but is not modeled in detail here.

Paroxysmal eruptions

Five paroxysmal, long-duration eruptions occurred during the observation period (Fig. 2). The eruptions began with intermittent periods of weak gas chugging that built into continuous chugging and finally louder explosions every 0.5–3 s that persisted for 24–48 h. The continuous explosions fueled sustained eruptive plumes of gas and fine ash, which developed quickly after the onset of each eruption. The plumes rose 1–4 km above the summit crater and stretched 15–25 km in the downwind direction (Fig. 4). A period of lava effusion always preceded the paroxysmal eruptions, and continued until the end of each eruption.

Similar eruptions in the current period of activity have been classified as strombolian (Smithsonian Institution 1999). However, the eruptions observed during 2005–2007 contained elements of both classic strombolian- and hawaiian-type eruptions and may be better described as transitional eruptions following the work of Parfitt and Wilson (1995) and Parfitt (2004). The 1973 eruption of Heimaey volcano also displayed this type of eruptive activity with explosions 0.5–2 s apart that produced a sustained eruption cloud reaching 6–10 km and continuous lava effusion (Blackburn et al. 1976).

Paroxysmal eruptions were spectacular at night, spraying clots and curtains of incandescent magma 50–300 m above the crater (Fig. 5). During the most energetic periods of activity, nearly overlapping explosions produced sustained fountains of incandescent ejecta. The explosions were clearly heard 15 km from the summit, and the strongest explosions produced shock waves that rattled windows and metal roofs 8 km from the summit. Increased lava effusion during paroxysmal eruptions (Fig. 2) frequently produced simultaneous flows in three to five of the canyons on the southern half of the cone. Lava effusion peaked during the most energetic explosive activity and terminated abruptly at the end of every paroxysm (Fig. 2).

During four of the five paroxysmal eruptions observed, a second vent on the southwestern flank ~100 m below the

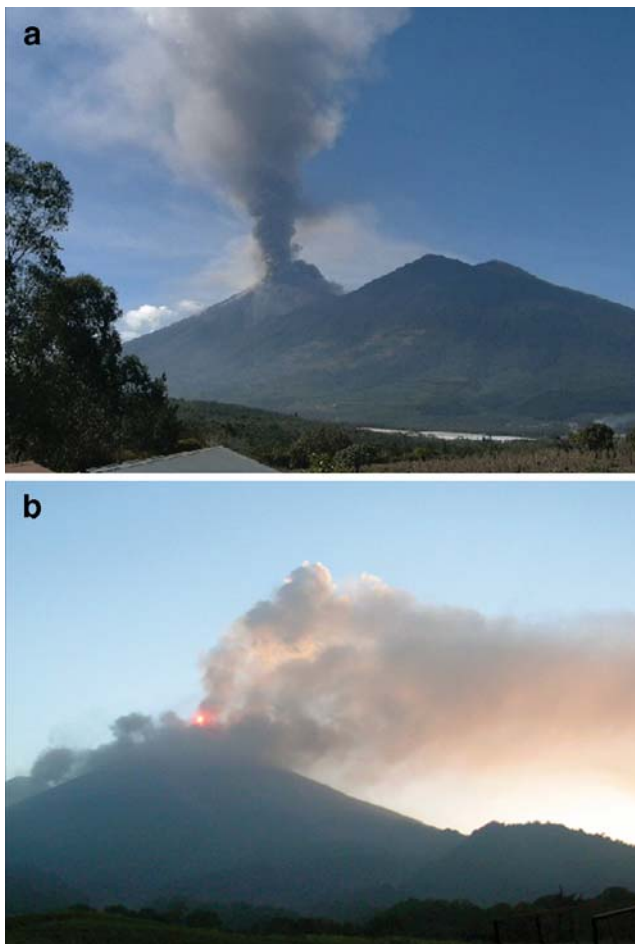


Fig. 4 Photographs from paroxysmal eruptions of Fuego during the study period. A: 27 December 2005 (view is to the west from the town of Alotenango ~10 km from summit), notice small pyroclastic flow moving north from the base of the eruptive column. B: 16 March 2007 (view is to the northeast from observatory), notice overriding ash cloud from a small block and ash flow descending down Barranca Seca (left of eruptive column)

summit vent (Fig. 5) produced a lava flow and explosions every 2–5 s. Explosions and lava effusion always continued from the main crater when the flank vent was active but the timing of explosions at the two vents did not coincide.

Fuego's paroxysmal eruptions are capable of producing pyroclastic flows that could reach several villages within 5–15 km of the vent and are the most significant hazard at the current level of activity. All of the eruptions observed during 2005–2007 produced block and ash flows that developed from the downslope fronts of active lava flows. Nighttime observations during the eruption of 26–27 June 2006 showed that small pyroclastic flows would begin near or at the front of active lava flows several hundred meters below the summit. A small area near the front of the flow grew dark at the onset of each collapse, with the ash cloud quickly engulfing the entire summit. Careful observations showed that lava flow growth was aided by agglutination of

still-plastic pyroclasts falling onto the upper reaches of the lava flow (Head and Wilson 1989). Loading of the near-vent portion of the lava flows through this process may have triggered a given lava flow to collapse and form pyroclastic flows (Head and Wilson 1989).

Velocities of pyroclastic flows that accompanied the 26–27 June 2006 paroxysm ranged from 25 km/hr to as high as 150 km/hr. During peak activity, a pyroclastic flow generated at the front of an active lava flow traveled 5 km down the Barranca Ceniza in 2 min. Near the end of the paroxysm, a small block and ash flow began as a lava flow

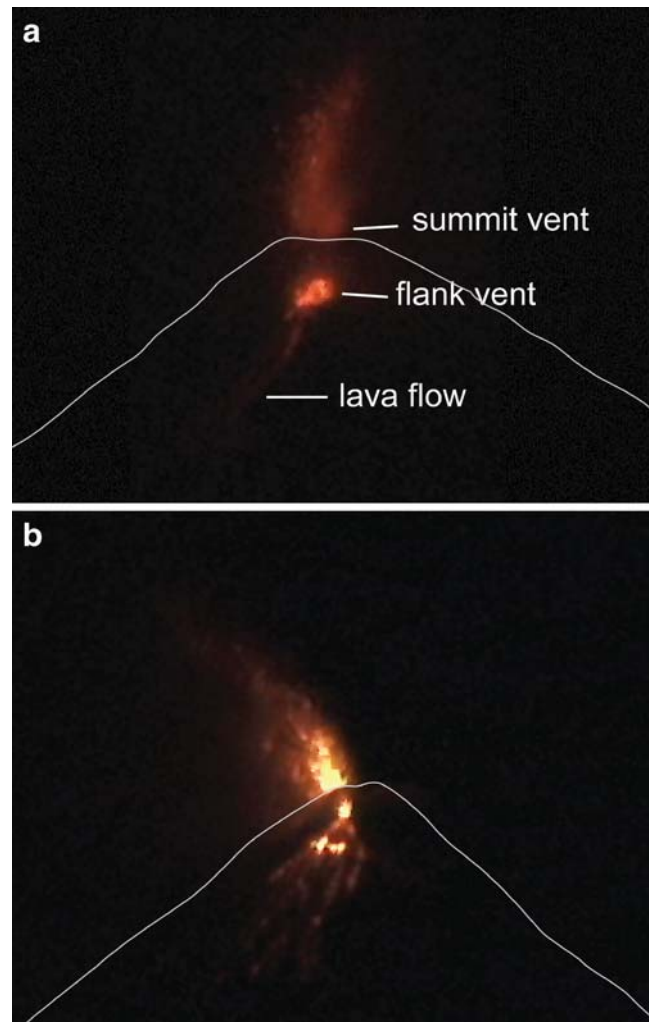


Fig. 5 Nighttime images of paroxysmal eruptions at Fuego taken from a video camera at the INSIVUMEH observatory 7.5 km from the summit crater (Fig. 1). The first image is focused on just the upper portion of the cone, while the second image has a wider viewing angle. White line outlines the profile of the upper cone A: 15 March 2007 eruption with incandescent ejecta reaching ~250 m above the summit crater. The primary summit crater vent and the flank vent were simultaneously active during the eruption. The flank vent was located ~100 m below the summit in the direction of Barranca Taniluya. B: 1 July 2007 eruption with both vents active. Bubble bursts and a lava flow emanated from the flank vent and deposited material in Barranca Taniluya

front collapsed several hundred meters below the summit. The thin, narrow pyroclastic flow descended several hundred meters, came to rest, then was remobilized tens of seconds later and descended several hundred meters more. This pattern repeated several times as the flow slowly descended over 4 km in 9 min.

Although paroxysmal eruptions always followed periods of lava effusion and minor strombolian explosions, neither our group nor the local volcano observers from INSIVUMEH were able to unequivocally forecast their onsets. Increased audible chugging always preceded these eruptions, but increases in the intensity and duration of chugging often occurred without a subsequent eruption. Likewise, increased incandescence (seen at night) from the summit crater always preceded an eruption, but was commonly followed only by minor increases in lava flow length.

The eruptions began very rapidly with the onset of sustained explosions that ejected pyroclasts from the summit crater. The end of the eruptions were nearly as abrupt, often starting with a decline in the intensity and frequency of explosions and a decrease in the amount of ash in the plume and then a decrease in the length of lava flows and occurrence of pyroclastic flows. When activity began to decrease, it typically took several hours to reach complete quiescence. Following an eruption, Fuego was typically quiet for several days, producing only a passive degassing plume prior to the onset of the degassing explosions.

Degassing explosions

The explosions that occurred during periods of effusion were distinct from those produced when no lava flows were active in terms of audible volume and frequency, ash content, size of explosion cloud, and frequency of occurrence. Explosions in the absence of lava effusion, which we term degassing explosions, were typically louder, more ash-rich, ejected more ballistics, and occurred less frequently than explosions during lava effusion. Discrete degassing explosions began within days of the end of a paroxysmal eruption, (Fig. 6) and lasted for about a week. Dark grey explosion clouds exited the summit crater at a rate of 1–5 per hour and quickly rose several hundred to 2,000 m above the summit. The explosions were not audible 7.5 km from the summit; the audible acoustic energy may have been absorbed or muffled by debris from the previous paroxysmal eruption overlying the fragmentation zone as suggested by (Murata et al. 1966) and (Mori et al. 1989).

The short period of silent, ash-rich explosions evolved to less ashy, but much noisier blasts. Grey to bluish-white eruptive clouds from these events rose hundreds of meters above the summit crater and, ~20 s after the visible onset of the explosion, a loud report was heard at 7.5 km from the summit. The loudest explosions were heard 21 km from the



Fig. 6 Photograph of a large degassing explosion on 21 March 2007 at 0728 h local time, 5 days after the end of the 15–16 March paroxysmal eruption and quiescence of lava effusion. View is to the northeast from the observatory. Column is ~2,000 m height above the summit. A weak audible report accompanied this explosion. Similar explosions during this period caused short periods (3–5 min) of ashfall up to 10 km from Fuego

summit, while the accompanying shock wave rattled windows and shook metal roofs up to 12 km from the summit. As the transition from degassing explosions to lava effusion began, explosions would become more frequent and increasingly ash-rich. In some cases, short periods of weak gas chugging would follow explosions. At night, an incandescent pulsing or flashing within the crater accompanied the chugging and could be seen projected in the degassing plume above the summit. As magma neared the surface, the explosions (observed at night) threw incandescent pyroclasts above the summit and generated minor rockfalls. Renewed effusion began with increased incandescent rockfall generated at some point on the rim of the summit crater, probably the low point where the crater was no longer able to contain the new lava. Within days of the appearance of a sustained lava flow, the ash content of the explosions decreased significantly and the explosions changed from muffled blasts to shorter, sharper reports signaling a return to the passive lava effusion stage.

Data overview

Lava flow length and mean daily lava output rate

The eruption characterization described was derived from visual observations. Daily lava flow lengths are estimated by summing the total lengths of all active lava flows visible to the authors with those reported by INSIVUMEH observers from different sectors of the volcano. Lava flow lengths were estimated from a scaled profile of the volcano

drawn on an observatory window. Repeated measurement of active lava flow lengths by JJL and the two volcano observers routinely resulted in agreement of ± 50 m. While somewhat qualitative, they are the only data consistently available for the whole of the observations reported here.

A fixed cross-sectional area of 60 m^2 was used for all lava flow volume calculations based on widths of flows measured in aerial photos and observed in the field, and thicknesses of flows observed in the field. The daily lava flow length multiplied by the cross-sectional area is then divided by a complete day to produce a mean daily lava output rate (Harris et al. 2007). This approximation most likely overestimates the cross-sectional area of shorter flows by up to a factor of 3 and underestimates the cross-section of longer flows, especially during paroxysmal eruptions, up to a factor of 3. We assume that the entire volume of the lava flow from the previous day is destroyed by calving of that flow, thereby allowing us to use the whole length from any given day rather than the difference between lengths observed on that day and the previous day. Basaltic flows emplaced on steep slopes ($>30^\circ$) at Stromboli have been shown to lose up to 70% of their erupted volume due to flow front collapse (Lodato et al. 2007). Our assumption of total loss by collapse probably overestimates the amount of calving by at least 30%.

Calving was the primary indication of the location of active flow fronts. We assume that calving is a direct result of magma flux into the head of the flow. If a flow was not observed to be shedding blocks, we assumed that input had stopped, and that the output rate was zero. A more detailed set of observations and a higher sampling rate are necessary to reduce the assumptions we make here and better constrain the calving rate, which is an important factor to include in output or effusion rate calculations for volcanoes that emplace flows on steep slopes.

Thermal output

Thermal alerts for volcanoes worldwide are obtained from NASA's moderate resolution imaging spectroradiometer (MODIS) through the automated volcanic thermal alert algorithm MODVOLC (Wright et al. 2002a, 2004). Low-spatial-resolution, high-temporal-resolution thermal data from MODIS has been used successfully to remotely monitor new and ongoing volcanic eruptions worldwide (Flynn et al. 2002; Patrick et al. 2005; Wright et al. 2005). On average, one satellite image is acquired every 12 h. The MODVOLC algorithm uses differences in short-wave radiation ($4 \mu\text{m}$) emitted by hot volcanic deposits (bands 21 and 22), and long-wave radiation ($11 \mu\text{m}$) from background surfaces (band 32) to determine anomalous hot spots at georeferenced volcanoes worldwide (Wright et al. 2002a). The resultant hot spots are posted to a website (<http://modis.higp.hawaii.edu/>) in near-real-time. Radiative

heat flux was determined from spectral radiance via a simple empirical relationship described in detail in Kaufman et al (1998) and Wright and Flynn (2004). Our heat flux calculations use only nighttime data in order to avoid a potential source of error from solar reflections and solar heating (Wright and Flynn 2004).

The MODVOLC algorithm is tuned to rapidly detect volcanic hotspots worldwide and there are limitations for using the data to estimate heat output. Short, narrow lava flows produced by Fuego during parts of the study may fall below the detection limit of MODVOLC and not trigger an acquisition. Furthermore, visual images are not co-collected with each hotspot acquisition so it is difficult to assess the effects of atmospheric clouds and eruption plumes on the spectral data. No other ground-based or satellite-based thermal data are available for Fuego and no error estimates for MODVOLC data are published so we can not quantify error in the heat loss calculation. However, Wright and Flynn (2004) show that the heat flux determined from the MODVOLC data at Erta Ale are consistent with both short-term ground-based measurements and longer-term satellite data using different methods. It is important to note that we are using the radiative heat output as a relative, long-term metric of eruption intensity to compare with our observational data, and to not attempt to model the flux directly.

Seismic and acoustic data

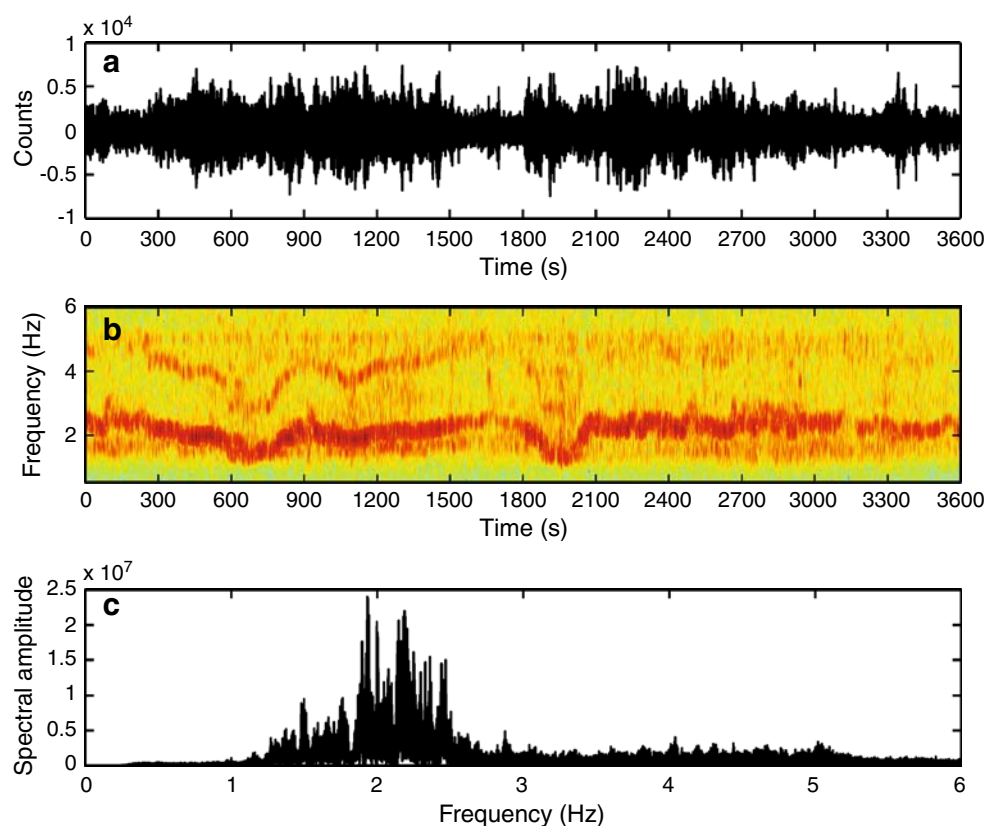
A seismo-acoustic station installed ~ 7 km southwest of the summit of Fuego during the last 6 months of the study period consisted of a Geospace GS-1 short-period vertical seismometer and two low-frequency microphones (Fig. 1). Data were recorded nearly continuously from 16 January–7 July 2007 (172 days). Time and frequency-domain analysis of seismic records from the entire data set showed that volcanic tremor between 1 Hz and 3 Hz was present during all three periods of eruptive behavior (Fig. 7), similar to well-documented tremor at other volcanoes with persistent basaltic eruptions (e.g. Pavlof (McNutt 1986); Stromboli (Falsaperla et al. 1998); Etna (Alparone et al. 2007)). Three periods of lava effusion and strombolian explosions, three paroxysmal eruptions, and two complete periods of degassing explosions occurred while the seismo-acoustic station was operating (Fig. 8).

Data analysis

Lava flow lengths and thermal output (August 2005–July 2007)

Fuego effused visible lava flows from the summit crater for 461 (63.2%) out of the 730 days of the study period, while

Fig. 7 Waveform (a), spectrogram (b), and spectrum (c) of a representative hour of harmonic tremor from Fuego recorded 13 June 2007. The seismic data were filtered between 0.5 Hz and 6 Hz, due the presence of an anthropogenic harmonic oscillator that produced signals in the 8–10 Hz range. Frequency content was determined by computing a fast Fourier transform (FFT) over the hour-long time series data in 500 sample (5 s) windows with a 250 sample (2.5 s) overlap between windows. The spectrogram (b) shows how the frequency glides over relatively short timescales, while the spectrograph (c) illustrates how harmonic tremor varied between 1 Hz and 3 Hz during the study period



for 266 days (36.8%) no effusion was observed (Fig. 1). Active flows shed blocks from the front and sides of the flow, which were visible as dust plumes during the day and incandescence at night. The average length of all lava flows active during periods of passive effusion and strombolian explosions (i.e., excluding paroxysmal eruptions) is 371 m. The average length of all the active lava flows during the paroxysmal eruptions is 1,960 m, or 5.3 times greater than during passive effusion. The average duration of effusive periods, including the paroxysmal eruptions, was 38.8 days, while periods of no effusion averaged 30.0 days long.

The observed lava flow length and the total radiant heat output correlate well for the duration of the study (Fig. 2). The radiant heat output dropped below the MODVOLC detection limit at nearly the same time as observed lava flow activity ceased and explosive activity changed after extended periods of effusion in 2005 and early 2006 (Fig. 2). This suggests that the lava flows produced during this period were relatively thin and cooled quickly, which agrees with proximal flow characteristics in aerial photos and our observed estimate of lava flow dimensions. The MODVOLC heat output estimates correlate with the rapid increases in lava flow length for four of the five paroxysmal eruptions (Fig. 2). The 20–21 June 2006 paroxysm was not detected by MODVOLC, but this eruption occurred during the rainy season in Guatemala, and the volcano was cloud-covered for much of the eruption. Similar to the observed

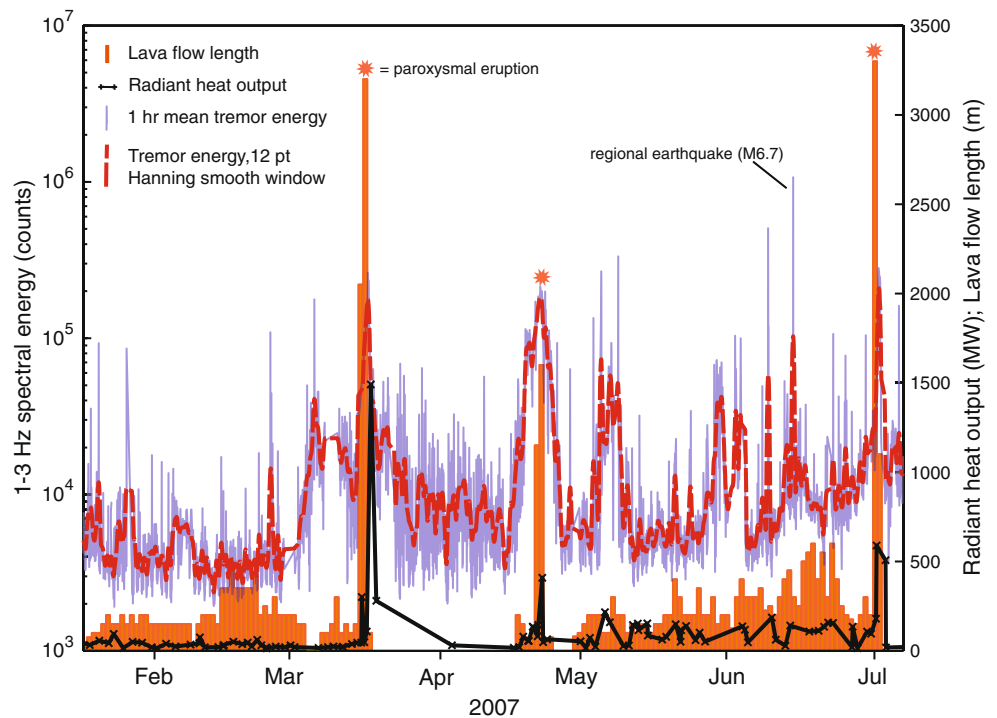
lava flow lengths, radiant heat outputs increase rapidly at the onset of paroxysms and then decrease rapidly at their conclusions. Beginning late in 2006, spikes in MODVOLC data occurred during periods when no lava flow activity was observed (Fig. 2). High radiant heat measurements during periods with no observed effusion, along with increasingly shorter periods of lava quiescence and more frequent paroxysmal eruptions in the second half of the study, may indicate that the free surface of the magma column remained closer to the surface during this period compared to the first half of the study.

Mean daily lava output rate (August 2005–July 2007)

On the basis of the lava flow length data and estimated cross-sectional area, we were able to make an estimate of the mean daily lava output rate (Fig. 9). This nomenclature follows the work of Harris et al. (2007) and is useful because it provides a metric of eruption intensity, assuming that calving completely destroys the lava flow each day.

The time-averaged bulk rock output rate during the entire study period is $0.18 \text{ m}^3 \text{ s}^{-1}$; however, the rate varied by more than two orders of magnitude between the lowest and highest daily mean output rates, $0.021 \text{ m}^3 \text{ s}^{-1}$ and $2.43 \text{ m}^3 \text{ s}^{-1}$, respectively. Our output values are similar to longer-term bulk rock discharge rates at the two other continuously active volcanoes in Guatemala. From 1954–

Fig. 8 Lava flow lengths (orange bars), radiant heat output (black), and tremor energy (blue and red) from 16 January–7 July 2007. Vertical bars represent daily total active lava flow lengths (right axis label), as in Fig. 2. Radiant heat output (black line with crosses; right axis label) determined from MODIS, as in Fig. 2. Faint blue trend is the hourly mean seismic energy calculated only in the 1–3 Hz band (left axis label). A 12-point Hanning smoothing window was applied to the hour-long mean seismic energy data (dashed line). Paroxysmal eruptions on 15–16 March, 20–21 April, and 1–2 July (asterisks) were recorded clearly in all three datasets



2001 the time-averaged discharge rate at Santiaguito volcano was $0.38 \pm 0.08 \text{ m}^3 \text{ s}^{-1}$, while at Pacaya volcano the time-averaged discharge rate was $0.22 \pm 0.02 \text{ m}^3 \text{ s}^{-1}$ from 1961–2001 (Durst et al. *in review*). The 2002–2003 effusive eruption of Stromboli volcano had many characteristics similar to Fuego's ongoing activity. The time-averaged discharge rate for that eruption was $0.32 \text{ m}^3 \text{ s}^{-1}$ with a measured variation of $0.1\text{--}0.7 \text{ m}^3 \text{ s}^{-1}$ (Lodato et al. 2007).

Based on our output rate, the total volume of lava produced during this period is $11.3 \times 10^6 \text{ m}^3$. This estimate does not include tephra deposits, which may be significant during the paroxysms, because most tephra were deposited on inaccessible portions of the cone. The most recent georeferenced aerial photographs from Fuego are available from 2001 and 2006. Using the photos and our knowledge of where most of the deposition has occurred in recent years, we were able to delineate an area of maximum growth of the upper cone. We estimate a uniform thickness of new material of between 10 m and 50 m on the basis of measureable landforms, which gives a total volume increase of $9\text{--}48 \times 10^6 \text{ m}^3$ over 6 years. Assuming a steady rate of growth, the volumetric growth of the upper cone during the study period would be $3\text{--}16 \times 10^6 \text{ m}^3$, which is comparable to our volume estimate from the output rate.

Seismicity, lava flows, and thermal output, January 16–July 7, 2007

Installation of the seismo-acoustic station in 2007 provided another means to track volcanic activity quantitatively and

improved the temporal resolution of monitoring at Fuego. We used spectral energy in the 1–3 Hz band to quantify tremor energy. The typical dominant tremor frequency was 2 Hz, but the wider band was chosen so we would capture all the energy during gliding episodes (Fig. 7). One or more overtones of this fundamental frequency were occasionally observed. In order to examine the entire dataset, we computed hourly means of spectral energy in this band. Overall, tremor energy correlates well with both the observed lava flow lengths and the thermal output, except during degassing explosions (Figs. 8, 10). The paroxysmal eruptions are recorded in the tremor energy, as peaks 10–50 times larger than the background tremor energy. These peaks coincide with spikes in thermal output and lava flow lengths. Peak tremor energy is similar for the three paroxysms, but the shapes of the tremor amplitude spikes vary (Fig. 8).

During the 2000 Southeast Crater eruption of Mt. Etna, Alparone et al. (2003) observed one of three patterns of tremor amplitude increase and decay during 62 of 64 lava fountaining episodes. Different patterns dominated during different stages of the eruption suggesting they were characteristic of specific states of the magmatic system. We recorded two distinct tremor evolution patterns during three paroxysms at Fuego. The 15–16 March eruption, which showed the longest increase in background tremor energy (~ 20 days) and had a higher intensity spike during the 2 days of paroxysmal activity, is similar to the tower-shaped events of Alparone et al. (2003) that dominated toward the end of the Etna eruption. While our record of the July paroxysm is incomplete, it appears similar to the

March eruption. These tower events indicate a rapid change in the activity. The 20–21 April eruption shows a shorter (~10 days), smoother increase and decrease in tremor energy symmetric about the 2 days of paroxysmal eruption, similar to bell-shaped events that dominated the beginning and middle phases of the 2000 Etna eruption. If more events can be recorded and studied at Fuego, these changes in tremor morphology may become useful for modeling the variable source processes.

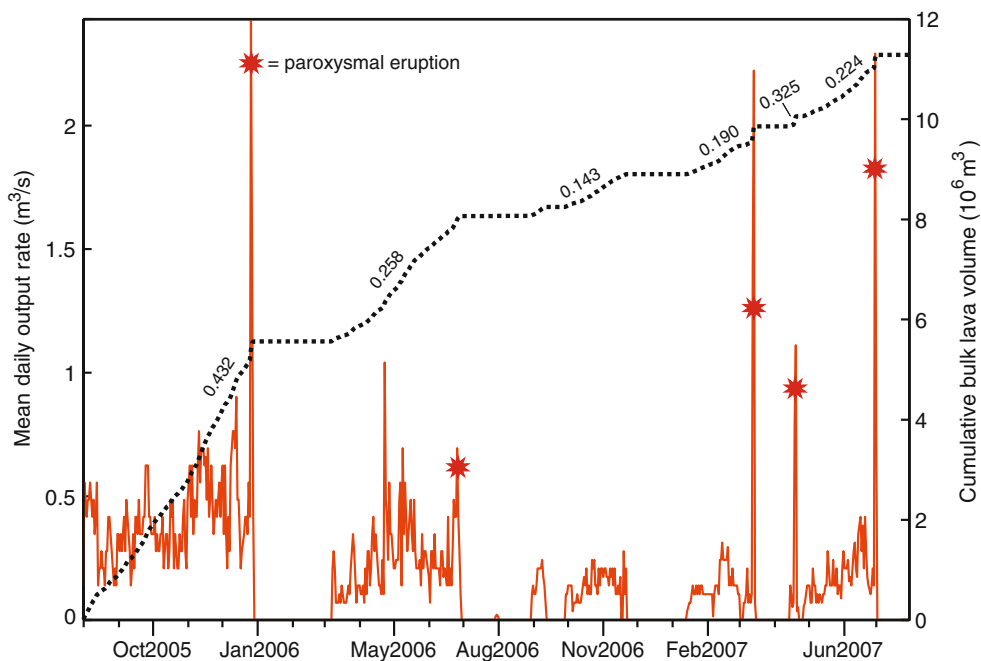
The similarities in lava flow length and thermal output for the March and July paroxysms highlight differences between these events and the April paroxysm. Maximum lava flow lengths for the April event were half those observed for both the March and July eruptions, while the thermal output of the March event was nearly four times greater than that of the April event. Lava flow length and tremor energy are remarkably similar for the March and July eruptions, although the thermal output appears to be significantly lower for the paroxysmal July eruption. This is likely due to the fact that the July eruption occurred during the rainy season, and significant cloud coverage was observed during the eruption, whereas the March and April eruptions were cloud-free.

Tremor energy spiked several times during periods of passive effusion to levels approaching those associated with paroxysmal eruptions. The majority of these spikes are due to tremor bursts that are similar in spectral content and waveform to the intense tremor that is characteristic of all paroxysmal eruptions. Several short-lived spikes in Fig. 8 are due to regional or teleseismic earthquakes that produce energy in the tremor band. The largest spike in tremor energy not associated with a paroxysmal eruption occurred

at the beginning of May 2007, concurrent with the onset of a period of lava effusion that lasted until the 1 July, 2007 eruption (Fig. 8). The similarity between the seismic signal of a paroxysmal eruption and that of passive effusion suggests that these two different types of activity are driven by magma migration and/or gas release in the plumbing system at Fuego. Subtle spikes in the thermal output also typically accompany the increases in tremor energy, although they are much weaker than the thermal output recorded during paroxysmal eruptions. This is further evidence that the tremor at Fuego is directly related to magma migration in the conduit.

Frequency gliding in volcanic tremor has been identified at a number of volcanoes worldwide (e.g., Arenal, Karymsky, Montserrat, Lascar, Sangay, Semeru). Gliding occurs when the fundamental tremor band, and any corresponding overtones, undergo equal shifts in frequency with time (Benoit and McNutt 1997; Garcés et al. 1998; Lees et al. 2004). Gliding occurs throughout the seismic record during the study period at Fuego, and during all three types of eruptive activity identified. It was observed most often prior to and following paroxysmal eruptions (typically ~1 week before or after). Gliding and harmonic tremor are found less frequently in the acoustic record, only occurring simultaneously with tremor gliding in the seismicity. Garcés et al. (1998) observed similarity in seismic and acoustic tremor and gliding at Arenal, suggesting it reflects strong coupling of the magma's free surface with the atmosphere. Gliding has been attributed to repeatable changes in physical properties of the melt (i.e., bubble concentration) over short timescales due to degassing events or explosions, changes in the length of a

Fig. 9 Mean daily lava output rate (orange line) and cumulative erupted volume (dotted line) from August 2005–July 2007. Slope of each major period of effusion, including the paroxysmal events (asterisks), is the number shown above the cumulative trend



magmatic resonator, or pressure fluctuations (Julian 1994). At Karymsky and Sangay, gliding has been attributed to systematic increases or decreases in time between chugging events (Lees et al. 2004; Lees and Ruiz 2008). Increasing frequency gliding at Fuego most often correlates with decreasing tremor amplitude, but sometimes the opposite effect is seen. A detailed examination of gliding at Fuego will be presented elsewhere.

The cumulative tremor energy, cumulative active lava flow length, and cumulative thermal output (Fig. 10) mirror the general agreement among the three datasets demonstrated earlier. Subtle changes in tremor energy during passive lava effusion can sometimes be correlated with small changes in thermal output, which cannot always be seen in lava flow data (i.e., several increases during May). Paroxysmal eruptions are associated with sharp increases in each parameter, while periods with no lava effusion show no thermal output. Cumulative tremor energy is continuous during periods without lava effusion and remains nearly the same as during passive effusion. Continued tremor with no effusion suggests that tremor is not due to magma flow, but that the magmatic system is still resonating strongly, likely due to a gas-charged magma column residing at a shallow depth below the vent (Chouet 1985). The characteristics of the degassing explosions produced during periods without lava effusion (Johnson et al. 2004; Lyons et al. 2007) support the model of a closed or choked vent, in which gas overpressure can build above the degassing magma column.

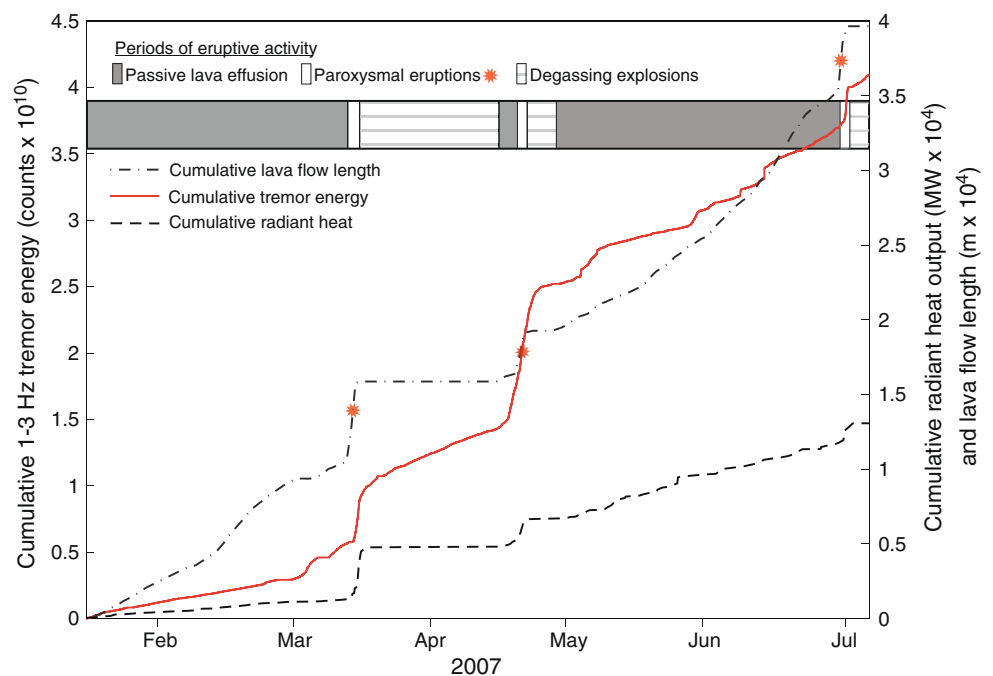
The sharp increase in cumulative tremor energy, thermal output, and lava flow length scale proportionally for the

March and July paroxysmal eruptions (Fig. 10). The 21 April paroxysm, however, produced significantly more tremor energy than commensurate with the observed lava flow length or the thermal output, and twice that of either the March or July eruptions. Because both the lava flow length and the thermal output are controlled by the amount of magma erupted at the surface, the data imply that less magma was erupted during the April eruption than during either the March or July eruptions. Having less magma erupt during a seismically more energetic eruption is not expected, but may be caused by the release of more gas and less magma relative to the other paroxysms. A choked or restricted conduit that somewhat restricted the flow of magma but allowed gas to escape could be envisaged.

Infrasound

Infrasound recordings complement seismic data for studying the variability and evolution of volcanic explosions and for monitoring changes in eruptive behavior. Relatively simple paths from sources to receivers, compared to seismic recordings, permit more direct interpretations of infrasound data (Vergnolle and Brandeis 1994; Buckingham and Garcés 1996; Johnson et al. 1998). The infrasound record quantifies the observations of explosions described above. Explosions are more frequent and have lower peak-to-peak amplitudes during periods of effusion. Periods without effusion typically have fewer but higher-amplitude degassing explosions. Degassing explosions have impulsive onsets interpreted as rapid outward expansion of trapped gas (Fig. 11a). The coda of ash-poor explosions decays

Fig. 10 Cumulative tremor energy (*red*), radiant heat output (*dashed*) and lava flow lengths (*dot-dash line*) from 16 January–7 July 2007, and observed periods of activity (*bar above*)



rapidly (Fig. 11a); these explosions are associated with a small explosion cloud primarily composed of gas. Ash-rich degassing explosions continue to vent gas and ash for tens of seconds and have an extended infrasonic coda following an impulsive onset. Johnson et al. (2004) proposed the fragmentation of a pressurized foam layer as the mechanism for producing the extended infrasound signal.

Explosions that occur several times per hour during effusion often have an impulsive onset and short, tremor-like coda (Fig. 11b). These explosions are superimposed on a nearly continuous tremor-like signal that may represent degassing processes such as chugging or jetting. Explosions observed during effusive periods always ejected incandescent material and gas but produced very little ash. The explosions are most likely due to bubbles rising through the magma column and bursting at the free surface of the magma in the summit crater. The two examples shown in Fig. 11 are representative events from a period of degassing explosions (Fig. 11a) and a subsequent period of lava effusion (Fig. 11b). The pressure amplitude is reduced to a distance of 1 km from the summit, assuming spherical spreading of acoustic energy where amplitude decays as the inverse of distance from the volcano. Johnson et al. (2004) recorded explosions from Fuego in 2003, with reduced pressures of up to 100 Pa that sounded like distant thunder at 2.6 km. The explosion we recorded in Fig. 11a rattled windows and shook metal roofs with a loud crack that sounded like thunder directly overhead at a distance of 7.5 km from the summit. This suggests that the apparently low 21 Pa of pressure calculated for this event is a minimum value; the actual reduced pressure may be several times larger due to unmodeled path effects such as refraction.

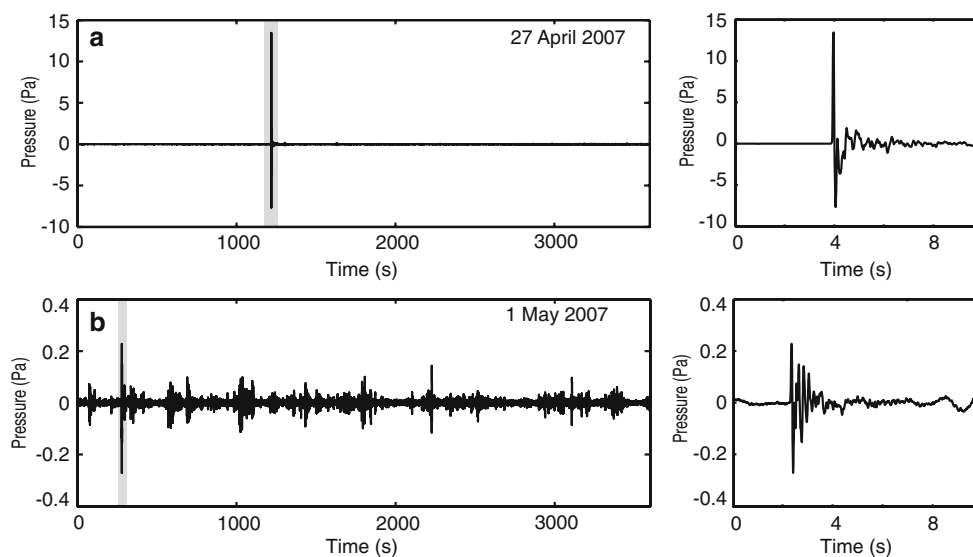
A dramatic change in the characteristics of explosions observed by infrasound accompanied the emergence of a new lava flow, first seen on 1 May 2007. The pressure

recorded at 7 km for the explosion on 27 April 2007 is 21 Pa, while on 1 May 2007 the pressure had dropped to 0.50 Pa, or 42 times less than 3 days prior. This corresponds directly to changes in the dynamics and processes acting in the upper conduit. Overpressure generated in the conduit can be many times greater during periods of degassing explosions than during passive effusion because the conduit is effectively sealed and significant amounts of gas can be trapped, possibly below a solidified cap of lava. During effusion, the conduit remains open, and gas bubbles can escape unimpeded through the free surface of the magma column at the summit, as small strombolian explosions. This demonstrates the utility of infrasound in monitoring activity at Fuego and supplies further quantitative support for our delineation of periods of activity based on observations.

Discussion

We found no documentation of the occurrence of regular, long-duration passive lava effusion (i.e., weeks to months) preceding paroxysmal eruptions at other basaltic arc volcanoes. A similar sequence was observed repeatedly, however, during the 1969–71 Mauna Ulu eruption of Kilauea volcano (Swanson et al. 1979), providing some insight into the eruptive behavior at Fuego. During the Mauna Ulu eruption, long periods of passive effusion preceded episodes of sustained lava fountaining that lasted from 4.5 h to 3 days. Following a fountaining episode, the lava column dropped below the lip of the vent and was often observed to be tens of meters below the vent. Over time the level would rise again and produce pahoehoe flows as it overtopped the vent, eventually leading to another fountaining event. The eruptive sequences observed at Fuego may be analogous to the progressions of activity

Fig. 11 Infrasound traces during periods of **a** degassing explosions and **b** lava effusion and minor strombolian explosions. Pressure amplitude is reduced pressure equivalent at 1 km from the source



during the Mauna Ulu eruption, with the magma chemistry and tectonic setting imparting significant temporal and behavioral differences during each period of activity.

Observed eruptive behavior of Mt. Etna is similar to activity we saw at Fuego. The 2000 Southeast Crater eruption of Mt. Etna consisted of 64 individual eruptive events that occurred in a sequential pattern of 1) slow effusion and gradual increase in strombolian explosions, then 2) paroxysmal eruption of sustained lava fountains that produced long lava flows and columns of gas and ash, and finally 3) decrease in volcanic tremor and return to strombolian activity followed closely by the end of the eruptive episode (Alparone et al. 2003). These events are similar to Fuego's eruptive sequences, with a key difference in eruptive cycle duration. Paroxysmal events at Etna were 20 min to 9 h in duration, whereas Fuego's paroxysms typically lasted 24–48 h and were preceded by weeks or months of passive effusion. Despite this difference, the similarities in tremor-dominated seismicity and cycles of eruptive behavior suggest that using Mt. Etna as an analogue to Fuego is constructive.

Fourier transform infrared spectroscopy (FTIR) performed at Etna during one paroxysm of the 2000 Southeast Crater eruption found that gas emissions during the eruption had higher ratios of CO_2/S and S/Cl than previous measurements at Etna, and could not be accounted for by simple bulk degassing of Etna basalts during the eruption (Allard et al. 2005). On the basis of this finding, Allard et al. (2005) invoke a model for Etnean paroxysms whereby a layer of volcanic gas accumulates at a structural discontinuity within the shallow plumbing system. The ascent and eruption of that gas pocket drives the paroxysms.

This model is similar to the foam layer model of Jaupart and Vergnolle (1988), whereby hawaiian and strombolian activity is driven by accumulation of gas in a foam layer at some structural discontinuity within the volcanic plumbing system. Moreover, they cite the characteristics of the 1969–71 eruption of Mauna Ulu (Kilauea volcano) in support of their experimental results. They propose that both passive effusion and paroxysmal phases of activity can be explained by 1) gas accumulation and growth of a foam layer allowing a period of slow effusion, followed by 2) collapse of the unstable foam layer into a gas slug that can move around the structural discontinuity and up the conduit, driving the fountaining upon its arrival at the surface. Evacuation of the foam layer at depth creates an available volume that may be filled by magma draining from the conduit. This is cited as the cause of rapid lava lake draining following the sixth fire fountaining episode in the Mauna Ulu eruption and may explain a period of decreased activity or repose following paroxysms (Vergnolle and Jaupart 1990). In this model, CO_2 is the primary volatile species accumulating at depth and creating

large bubbles, while H_2O only exsolves very small bubbles in the upper few hundred meters of the conduit (Vergnolle and Jaupart 1986).

The growth of a foam layer is controlled by gas flux and magma viscosity and must reach a critical thickness in order to collapse (Jaupart and Vergnolle 1989). If either liquid viscosity or gas flux is insufficiently high, then foam will flow passively around the chamber roof or structural discontinuity into the conduit resulting in continuous effusive behavior. However, if the viscosity or gas flux is sufficiently high, then cyclic foam growth and collapse will occur and could produce cycles of activity similar to those observed at Fuego.

An alternative model for generating the wide range of eruptions styles seen in basaltic systems is the magma rise-speed-dependence model (Parfitt and Wilson 1995). At low magma rise speeds, bubbles ascend and coalesce into larger bubbles that eventually reach the free surface of the magma and burst, producing classic strombolian activity. At higher magma rise speeds, nucleating bubbles have little differential movement relative to the magma, thus much less coalescence occurs. As the magma-gas mixture ascends, it reaches the ~75% volume exsolved gas threshold of fragmentation, or run-away coalescence, deeper within the conduit. The mixture continues to ascend and decompresses, accelerating rapidly to producing a hawaiian-style lava fountain. Increasing magma rise speeds would allow for a transition in eruptive behavior similar to that observed at Fuego (Parfitt 2004). With increasing magma rise speed, widely-spaced strombolian explosions would transition into more violent and frequent explosions, much like what we observed during the transition from passive effusion and strombolian explosions to paroxysmal eruptions at Fuego. Moreover, Parfitt and Wilson (1994) and Parfitt (2004) argue that the volatile species driving explosive basaltic activity is H_2O , not CO_2 as put forth by Vergnolle and Jaupart (1986).

A shift in activity appears to have occurred over the course of the study period that may provide insight into conduit dynamics at Fuego. Longer periods of passive effusion and fewer paroxysmal events towards the beginning of the study gave way to shorter periods of effusion and more frequent paroxysmal eruptions in 2007 (Fig. 9). Decreasing lava output occurs during the course of the study period, but explosivity increases. The overall decrease in output rate observed in Fig. 9 may indicate a changing conduit configuration. A lower magma flux through the conduit would result in narrowing of the magma pathway due to enhanced cooling, crystallization, and degassing at the conduit-wallrock interface (Gilbert and Lane 2008). Partial choking of the conduit could impede the upward migration of bubbly magma, which would decrease output rate. This process could cause gas-rich

magma to accumulate below the choked conduit, possibly forming a foam layer, similar to the model of Jaupart and Vergnolle (1988). Additionally, changes in the foam layer thickness due to variable deep gas flux or changing magma viscosity would contribute to temporal variations in the eruptive cycles observed. The inverse relationship between frequency of paroxysmal events and output rate is difficult to relate to the magma rise speed model because the model predicts that higher effusion rates should correlate with more paroxysmal eruptions, not lower effusion rate. If, as our data suggest, the volcano is becoming less open-vent in nature resulting in an increase in explosivity, it has significant hazard implications that warrant further research at Fuego.

Conclusions

We describe 2 years of daily observations of eruptive behavior at Fuego volcano, in an open-vent period of activity. The volcano was persistently active, and we observed a repeating cycle of activity: 1) passive lava effusion and minor strombolian explosion, followed by 2) paroxysmal eruptions, and finally 3) degassing explosions without lava effusion. A mean daily lava output rate of $0.18 \text{ m}^3 \text{ s}^{-1}$ was estimated from lava flow lengths. During paroxysmal events, the output rate increased by an order of magnitude. Thermal outputs from MODIS and active lava flow lengths show a robust correlation over the entire duration of the study. Our work shows that regular, systematic collection of observational data can be useful in tracking changes in volcanic activity, particularly in developing nations at populated volcanoes.

Continuous seismo-acoustic data was collected during the last 6 months of the study. Fuego produced constant, but variable-amplitude harmonic tremor during all three styles of eruptive behavior. Comparison of thermal output, tremor energy, and lava flow lengths during 2007 shows that all three data types correlate during periods of passive lava effusion and paroxysmal eruptions, but that tremor energy is emitted at the same level during periods of degassing explosions without effusion, as during periods of passive effusion. Tremor amplitude shows promise as an eruption forecasting tool if more eruptions can be recorded and a longer continuous record constructed and analyzed.

Of the three types of activity observed during the study, the paroxysmal eruptions are the most hazardous to local populations. Our data suggests the possibility that Fuego may be shifting toward less of an open-vent configuration, which could lead to an increase in the frequency of explosive events. More detailed studies of these events and improvements in monitoring would help elucidate their source processes and potentially assist local scientists in eruption forecasting.

Acknowledgements JLL would like to thank Eddy Sanchez, INSIVUMEH, and the Peace Corps for field support during the study period. The authors gratefully acknowledge Jeff Johnson for his field and equipment support and Rob Wright for MODVOLC data. The authors thank Rüdiger Escobar and Jose Palma for stimulating and insightful discussions. Thoughtful critiques by John Stix, Sonia Calvari and an anonymous reviewer improved the manuscript. This work was funded by NSF-PIRE 0530109 and the Peace Corps.

References

- Allard P, Burton M, Mure F (2005) Spectroscopic evidence for a lava fountain driven by previously accumulated magmatic gas. *Nature* 433:407–410
- Alparone S, Andronico D, Lodato L, Sgroi T (2003) Relationship between tremor and volcanic activity during the Southeast Crater eruption on Mount Etna in early 2000. *J Geophys Res* 108: B52241. doi:10.1029/2002JB001866
- Alparone S, Cannata A, Gresta S (2007) Time variation of spectral and wavefield features of volcanic tremor at Mt. Etna (January–June 1999). *J Volcanol Geotherm Res* 161:318–332
- Benoit JP, McNutt SR (1997) New constraints on source processes of volcanic tremor at Arenal Volcano, Costa Rica, using broadband seismic data. *Geophys Res Lett* 24:449–452
- Blackburn EA, Wilson L, Sparks RSJ (1976) Mechanisms and dynamics of strombolian activity. *J Geol Soc Lond* 132:429–440
- Buckingham MJ, Garcés MA (1996) Canonical model of volcano acoustics. *J Geophys Res* 101:8129–8151
- Calvari S, Spampinato L, Lodato L, Harris AJ, Patrick MR, Dehn J, Burton MR, Andronico D (2005) Chronology and complex volcanic processes during the 2002–2003 flank eruption at Stromboli volcano (Italy) reconstructed from direct observations and surveys with a hand held thermal camera. *J Geophys Res* 110:B02201. doi:10.1029/2004JB003129
- Carr MJ, Patino LC, Feigenson MD (2002) Petrology and geochemistry of lavas. In: Bundschuh J, Alvarado GE (eds) *Central America: geology, resources, and hazards*. Taylor and Francis, London, pp 565–590
- Chouet B (1985) Excitation of a buried magmatic pipe: a seismic source model for volcanic tremor. *J Geophys Res* 90:1881–1893
- Falsaperla S, Langer H, Spampinato S (1998) Statistical analyses and characteristics of volcanic tremor on Stromboli Volcano (Italy). *Bull Volcanol* 60:75–88
- Flynn L, Wright R, Garbeil H, Harris A, Pilger E (2002) A global thermal alert system using MODIS: initial results from 2000–2001. *Adv Environ Monit Model* 1:37–69
- Garcés MA, Hagerty MT, Schwartz SY (1998) Magma acoustics and time-varying melt properties at Arenal volcano, Costa Rica. *Geophys Res Lett* 25:2293–2296
- Gilbert JS, Lane SJ (2008) The consequences of fluid motion in volcanic conduits. *Geol Soc London Spec Pub* 307:1–10
- Harris AJ, Dehn J, Calvari S (2007) Lava effusion rate definition and measurement: a review. *Bull Volcanol* 70:1–22
- Head JW III, Wilson L (1989) Basaltic pyroclastic eruptions: influence of gas-release patterns and volume fluxes on fountain structure, and the formation of cinder cones, spatter cones, rootless flows, lava ponds and lava flows. *J Volcanol Geotherm Res* 37:261–271
- Jaupart C, Vergnolle S (1988) Laboratory models of hawaiian and strombolian eruptions. *Nature* 331:58–60
- Jaupart C, Vergnolle S (1989) The generation and collapse of a foam layer at the roof of a basaltic magma chamber. *J Fluid Mech* 203:347–380

- Johnson JB (2007) On the relation between infrasound, seismicity, and small pyroclastic explosions at Karymsky volcano. *J Geophys Res* 112:B08203. doi:10.1029/2006JB004654
- Johnson JB, Lees JM (2000) Plugs and chugs—seismic and acoustic observations of degassing explosions at Karymsky, Russia and Sangay, Ecuador. *J Volcanol Geotherm Res* 101:67–82
- Johnson JB, Lees JM, Gordeev EI (1998) Degassing explosions at Karymsky volcano, Kamchatka. *Geophys Res Lett* 25:3999–4002
- Johnson JB, Aster RC, Kyle PR (2004) Volcanic eruptions observed with infrasound. *Geophys Res Lett* 31:L14604. doi:10.1029/2004GL020020
- Julian BR (1994) Volcanic tremor: non-linear excitation by fluid flow. *J Geophys Res* 99:11859–11878
- Kaufman YJ, Justice CO, Flynn LP, Kendall JD, Prins EM, Giglio L, Ward DE, Menzel WP, Setzer AW (1998) Potential global fire monitoring from EOS-MODIS. *J Geophys Res* 103:32215–32238
- Lautze NC, Harris AJL, Bailey JE, Ripepe M, Calvari S, Dehn J, Rowland SK, Evans-Jones K (2004) Pulsed lava effusion at Mount Etna during 2001. *J Volcanol Geotherm Res* 137:231–246
- Lees JM, Ruiz M (2008) Non-linear explosion tremor at Sangay, Volcano, Ecuador. *J Volcanol Geotherm Res* 176:170–178
- Lees JM, Gordeev E, Ripepe M (2004) Explosions and periodic tremor at Karymsky volcano, Kamchatka, Russia. *Geophys J Int* 158:1151–1167
- Lodato L, Spampinato L, Harris A, Calvari S, Dehn J, Patrick M (2007) The morphology and evolution of the Stromboli 2002–2003 lava flow field: an example of a basaltic flow field emplaced on a steep slope. *Bull Volcanol* 69:661–679
- Lyons JJ, Johnson JB, Waite GP, Rose WI (2007) Observations of cyclic strombolian eruptive behavior at Fuego volcano, Guatemala reflected in the seismo-acoustic record. *EOS Trans AGU* 88(52), Fall Meet Suppl, V11C
- Martin DP (1979) The historical activity of Fuego volcano, Guatemala: constraints on the subsurface magma bodies and processes therein. MS thesis, Michigan Technological University, Houghton
- Martin DP, Rose WI (1981) Behavioral patterns of Fuego volcano, Guatemala. *J Volcanol Geotherm Res* 10:67–81
- Métrich N, Bertagnini A, Landi P, Rosi M (2001) Crystallization driven by decompression and water loss at Stromboli volcano (Aeolian Islands, Italy). *J Petrol* 42:1471–1490
- Métrich N, Allard P, Spilliaert N, Andronico D, Burton M (2004) 2001 flank eruption of the alkali- and volatile-rich primitive basalt responsible for Mt. Etna's evolution in the last three decades. *Earth Planet Sci Lett* 228:1–17
- McNutt SR (1986) Observations and analysis of B-type earthquakes, explosions, and volcanic tremor at Pavlof volcano, Alaska. *Bull Seismol Soc Am* 76:153–175
- Mori J, Patia H, McKee C, Itikarai I, Lowenstein P, De Saint Ours P, Talai B (1989) Seismicity associated with eruptive activity at Langila volcano, Papua New Guinea. *J Volcanol Geotherm Res* 38:243–255
- Murata KJ, Dondoli C, Saenz R (1966) The 1963–65 Eruption of Irazú volcano, Costa Rica (the period of March 1963 to October 1964). *Bull Volcanol* 29:765–796
- Parfitt EA (2004) A discussion of the mechanisms of explosive basaltic eruptions. *J Volcanol Geotherm Res* 134:77–107
- Parfitt EA, Wilson L (1994) The 1983–86 Pu'u 'O'o eruption of Kilauea volcano, Hawaii: a study of dike geometry and eruption mechanisms for a long-lived eruption. *J Volcanol Geotherm Res* 59:179–205
- Parfitt EA, Wilson L (1995) Explosive volcanic eruptions IX. The transition between hawaiian-style lava fountaining and strombolian explosive activity. *Geophys J Int* 121:226–232
- Patrick MR, Smellie JL, Harris AJL, Wright R, Dean K, Izbekov P, Garbeil H, Pilger E (2005) First recorded eruption of Mount Belinda volcano (Montagu Island), South Sandwich Islands. *Bull Volcanol* 67:415–422
- Roggensack K (2001) Unraveling the 1974 eruption of Fuego volcano (Guatemala) with small crystals and their young melt inclusions. *Geology* 29:911–914
- Rose WI, Anderson ATJ, Woodruff LG, Bonis SB (1978) The October 1974 basaltic tephra from Fuego volcano: description and history of the magma body. *J Volcanol Geotherm Res* 4:3–53
- Schindwein V, Wassermann J, Scherbaum F (1995) Spectral analysis of harmonic tremor signals at Mt. Semeru volcano, Indonesia. *Geophys Res Lett* 22:1685–1688
- Sisson TW, Layne GD (1993) H₂O in basalt and basaltic andesite glass inclusions from four subduction-related volcanoes. *Earth Planet Sci Lett* 117:619–635
- Smithsonian Institution (1979) Fuego volcano. *Bull Glob Volcanism Netw* 12(1,8)
- Smithsonian Institution (1999) Fuego volcano. *Bull Glob Volcanism Netw* 24(7)
- Swanson DA, Duffield WA, Jackson DB, Peterson DW (1979) Chronological narrative of the 969–71 Mauna Ulu eruption of Kilauea volcano, Hawaii. *US Geol Surv Prof Pap* 1056:1–55
- Vergnolle S, Jaupart C (1986) Separated two-phase flow and basaltic eruptions. *J Geophys Res* 91:12842–12860
- Vergnolle S, Jaupart C (1990) Dynamics of degassing at Kilauea volcano, Hawaii. *J Geophys Res* 95:2793–2809
- Vergnolle S, Brandeis G (1994) Origin of the sound generated by Strombolian explosions. *Geophys Res Lett* 21:1959–1962
- Wright R, Flynn LP (2004) Space-based estimate of the volcanic heat flux into the atmosphere during 2001 and 2002. *Geology* 32:189–192
- Wright R, Flynn L, Garbeil H, Harris A, Pilger E (2002a) Automated volcanic eruption detection using MODIS. *Remote Sens Environ* 82:135–155
- Wright R, Flynn LP, Garbeil H, Harris AJL, Pilger E (2004) MODVOLC: near-real-time thermal monitoring of global volcanism. *J Volcanol Geotherm Res* 135:29–49
- Wright R, Carn SA, Flynn LP (2005) A satellite chronology of the May–June 2003 eruption of Anatahan volcano. *J Volcanol Geotherm Res* 146:102–116